ISSN 2075-1133, Inorganic Materials: Applied Research, 2021, Vol. 12, No. 1, pp. 167–171. © Pleiades Publishing, Ltd., 2021.
Russian Text © The Author(s), 2020, published in Materialovedenie, 2020, No. 7, pp. 10–14.

Effect of Heating in the Intercritical Temperature Range on Formation of Austenite and Structure of Ultralow-Carbon Steel

O. V. Selivanova[a], *, O. N. Polukhina[a], V. A. Khotinov[a], A. Yu. Zhilyakov[a], A. S. Yurovskikh[a], G. V. Shchapov[a], and V. M. Farber[a]

[a] *Ural Federal University named after the first President of Russia B.N. Yeltsin, Yekaterinburg, 620002 Russia*
**e-mail: sov23@mail.ru*

Received October 28, 2019; revised February 3, 2020; accepted March 24, 2020

Abstract—Using micrographic, dilatometric, and high-temperature XRD methods, the kinetics of formation of austenite is studied under continuous heating of ultrafine-grained 08G2B steel in two initial states—after quenching and normalization.

Keywords: low-carbon steels, quenching, normalization, austenite formation, intercritical temperature range
DOI: 10.1134/S2075113321010366

INTRODUCTION

In recent years, the amount of research into formation of austenite under heating of steels in the intercritical temperature range has been steadily growing [1–5], since incomplete austenitization is increasingly often used as an intermediate or finishing operation for formation of the structural phase state of steels with a high combination of functional properties [4, 6–9]. To set precisely the chosen heat treatment conditions in the intercritical temperature range (ITR), a clear picture of the direction and intensity of the effect of both initial structural phase parameters and external factors (heating rate, temperature, and isothermal time) on the critical points, kinetics, and run of the $\alpha \rightarrow \gamma$ transition is necessary. An ultrafine grain size and microalloying with strong carbide formers may bring features to austenite formation, which currently is widely used in structural steels [10].

This predetermined the aim of the present work: to study the kinetics and structural behavior of formation of austenite and the level of the mechanical properties of ultrafine-grained 08G2B steel subjected to heating at different rates in the intercritical temperature range after normalization or quenching.

MATERIALS AND METHODS

In the work, industrially smelt 08G2B steel with the following chemical composition (wt %) was used: 0.08 C, ~2 Mn, 0.2 Mo, 0.02 Ti, 0.05 Nb, 0.02 V, 0.004 N, 0.04 Al, 0.004 S, and 0.007 P. The samples with a cross section of 10 × 10 mm were cut out of the middle of a 27.7-mm-thick sheet perpendicular to the rolling direction. After austenitization at 1000°C (for 30 min), they were subjected to quenching in water or normalization. To investigate the microstructure, the samples were heated in laboratory furnaces to 650, 730, 760, and 850°C at a rate of ~0.3°C/s without isothermal maintenance and quenched in water. Structural investigations were carried out on a NikonEpiphot 200 optical microscope and, with thin foils, on a JEM 2100 electron microscope. Dilatometric analysis was performed on an RITA L78 dilatometer (Linseis) at heating rates of 0.3 and 90°C/s. The amount of austenite formed under continuous heating at different rates, determined from the lever rule, was approximated by the Kolmogorov–Johnson–Mehl–Avrami equation

$$q_A = 1 - \exp\left[-k\tau^n\right], \quad (1)$$

where $\tau = T_i/V_h$ is the time for achieving temperature T_i under continuous heating at a rate of V_h, k is a constant; and n is the kinetic factor.

Function (1) is widely used in analysis of isothermal reactions; in the case of nonisothermal heating, it may be used for isokinetic reactions.

High-temperature X-ray diffraction investigations were conducted in an HTK1200N high-temperature chamber (Anton Paar) at a step of 100°C up to a temperature of 580°C and, next, at a step of 20°C up to 900°C in a vacuum (10^{-2} to 10^{-3} Pa). The carbon content in austenite was determined from the crystal lattice parameter

$$a_\gamma = a_{\gamma,0} + \alpha c_\gamma, \quad (2)$$

where a_γ and $a_{\gamma,0}$ are the lattice parameters of austenite formed in steel and in pure iron, respectively; c_γ is the

Table 1. Critical temperatures of 08G2B steel after heating at different rates: for numerator, $V_h = 0.3$°C/s; for denominator, $V_h = 90$°C/s

Pretreatment	Ac_1, °C	Ac_3, °C	A_{tr}, °C	ΔT_{ITR}, °C
Quenching	690/765	885/915	810/835	195/150
Normalization	—/765	—/925	—/830	—/160

carbon mass concentration; and α is the proportionality factor.

RESULTS OF INVESTIGATION

Dilatometric Investigations

These investigations showed that both the initial structure and heating rate have a noticeable effect on the critical points of the studied steel (Table 1). The heating rate is a quite strong factor: increasing the heating rate from 0.3 to 90°C/s leads to an increase in the critical points (Ac_1 by ~75°C and Ac_3 by ~30°C), which results in narrowing of the ITR (Table 1).

Description of the kinetics of austenite formation in the studied 08G2B steel allows one to classify the $\alpha \rightarrow \gamma$ transition as a diffusion-controlled isokinetic reaction [11]: at any point of time, the amount of formed austenite q_A is determined only by the rate of phase growth, which is proportional to the diffusion coefficient. For such reactions, nucleation of a new phase occurs at grain boundaries, which, as was demonstrated in [5], is satisfactorily implemented in the 08G2B steel in formation of austenite in the course of heating at the chosen rates.

Dependence (1) in linearizing coordinates $\ln\ln\frac{1}{1-y_A}$—$\ln\tau$ (Fig. 1) allowed us to recognize the stages of α–γ transformation, the kinetic coefficient n at each of them, and the temperature of transition A_{tr} from one stage to another.

It is seen that, independently of the initial state, the reaction of austenite formation consists of two stages: a rapid low-temperature one with $n_I = 1.0$ and a decelerated high-temperature one with $n_{II} = 0.5$. A change of stages weakly depends on the sample prehistory and occurs at a temperature of A_{tr} ~ 830°C (Table 1).

X-ray Diffraction Investigations

Analysis of the high-temperature XRD patterns (Fig. 2) revealed that, for the normalized sample, the temperature of the onset of γ-Fe formation is 700°C, and for the quenched sample, it is 750°C. The $q_A = f(T_h)$ curves have a form identical to that obtained by dilatometry.

From the XRD data, two stages of austenite formation are also separable; by the end of stage I, for the normalized sample, $q_A \approx 15\%$, and for the quenched sample, $q_A \approx 20\%$. In both samples, stage II starts at $T_h = 860$°C (close to A_{tr} obtained from the dilatometry data), and by 900°C, the austenite content reaches 97 to 100%. This is obviously connected with the number of defects of the crystal structure (dislocations) strongly fixed in the initial α phase by precipitates of

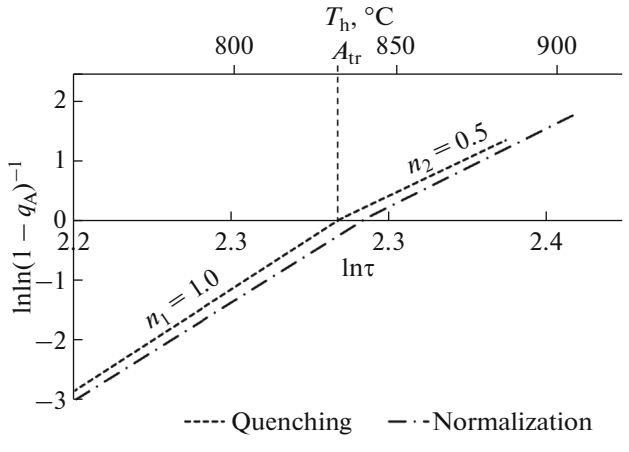

Fig. 1. Kinetic curves of austenite formation under continuous heating at rate of 90°C/s in linearizing coordinates and corresponding temperature scale (n_1 and n_2 are kinetic coefficients).

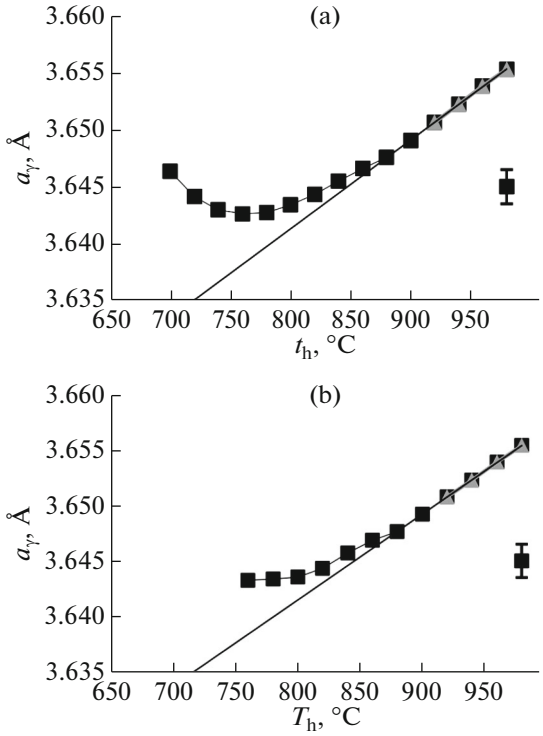

Fig. 2. Effect of heating temperature on crystal lattice parameter of austenite in investigated steel: (a) normalization and (b) quenching.

special carbides. An increase in the density of dislocations, which are places of easy diffusion, in the initially quenched sample leads to faster kinetics of austenite formation within the limits of low-temperature stage I compared to that in the normalized sample.

Changes in the lattice parameter of austenite Δa_γ (1) formed during heating are connected with the carbon content in it a_γ. Whereas Cr and Mn, because of closeness to an Fe atom in size, have a small effect on the behavior of Δa_γ, thermal expansion a_γ^T grows proportionally with an increasing temperature (Fig. 2). Then, $\Delta a_\gamma = a_\gamma - a_\gamma^T$.

Calculation of the high-temperature XRD patterns (Fig. 3) demonstrated that, in agreement with the Fe–C diagram, the first portions of austenite are appreciably rich in carbons, being more so in the initially quenched sample. With an increasing amount of formed austenite (heating temperature), the carbon content in it smoothly decreases, doing so more sharply in the initially quenched sample.

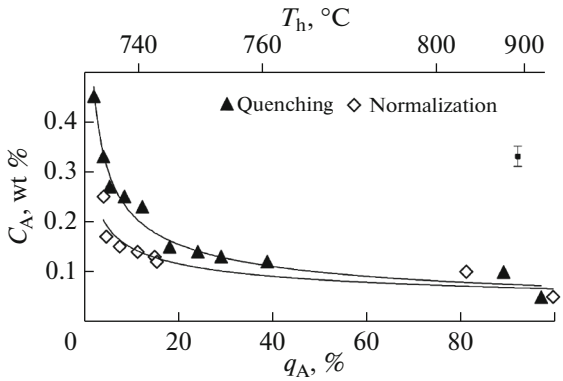

Fig. 3. Change in carbon content in austenite with increase in its amount.

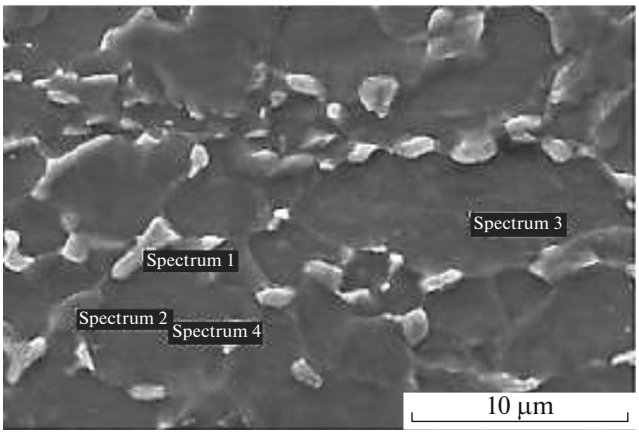

Fig. 4. Structure of 08G2B steel after heating to 700°C and cooling in air according to SEM data.

Investigation of Microstructure

Under heating to 1000°C, the investigated steel in in the austenitic region, and after quenching, the structure consists of packets of closely parallel α Fe laths, which are products of displacive transformations. After normalization, almost equiaxial grains of excess ferrite with rounded boundaries, on which small (~3 μm) areas of degenerate pearlite are located, are formed in steel [5]. After heating to 680–730°C, in the structure, there are ferrite grains (gray areas in the scanning electron microscopy (SEM) images) 3 to 10 μm in size and white rounded crystals of 0.3 to 1.5 μm in size along their boundaries, which may be considered as former grains of the formed austenite (Fig. 4). The same is indicated by an increase in their size and number with increasing temperature.

X-ray spectrum microanalysis of the areas designated as Spectrum in Fig. 4 showed that their chemical composition is close to the chemical composition of the studied steel in the main chemical elements. This made it possible to believe that first austenite grains, arranged in chains along the boundaries of the initial ferrite grains, are not noticeably rich in alloying elements. They are likely nucleated at the cementite/ferrite interfaces, where, owing to the minimum diffusion paths, the rate of formation of carbon-rich austenite is maximal.

Transmission electron microscopy investigations revealed that, after heating of the initially quenched steel to $T_h = 650$°C (lower than Ac_1), the lath structure persists in the samples, with the density of dislocations inherited from quenching being elevated in it (Fig. 5). On the dislocation lines, elongated curved particles of, probably, cementite with a length of up to 60 nm are observed together with rounded platelike particles of up to 5 nm (VC) in diameter according to the microdiffraction data (Fig. 5b). No dark-field images could be obtained owing to the weakness of their reflections, so they could not be those from residual austenite. The presence of residual austenite makes it clear that that the processes of its decomposition under this high-temperature tempering did not come to completion, which indicates the high thermal stability of the structural phase state in the studied steel.

After heating to $T_h = 760$°C (a little higher than Ac_1), the lath structure inherited from quenching persists in the samples (Fig. 6a). However, in some microvolumes, bulging areas of lath boundaries are seen already, which is evidence of their migration, together with new rounded crystals ~1.5 μm in size (Fig. 6a). Comparison between the rounded crystals and the first formed rounded austenite grains (Fig. 4) enables one to suggest that they are identical, although, in the electron diffraction pattern (Fig. 6b), there are only α-Fe reflections. The formed austenite is likely to have been transformed into ferrite upon cooling, with carbon atoms pushed off to the periph-

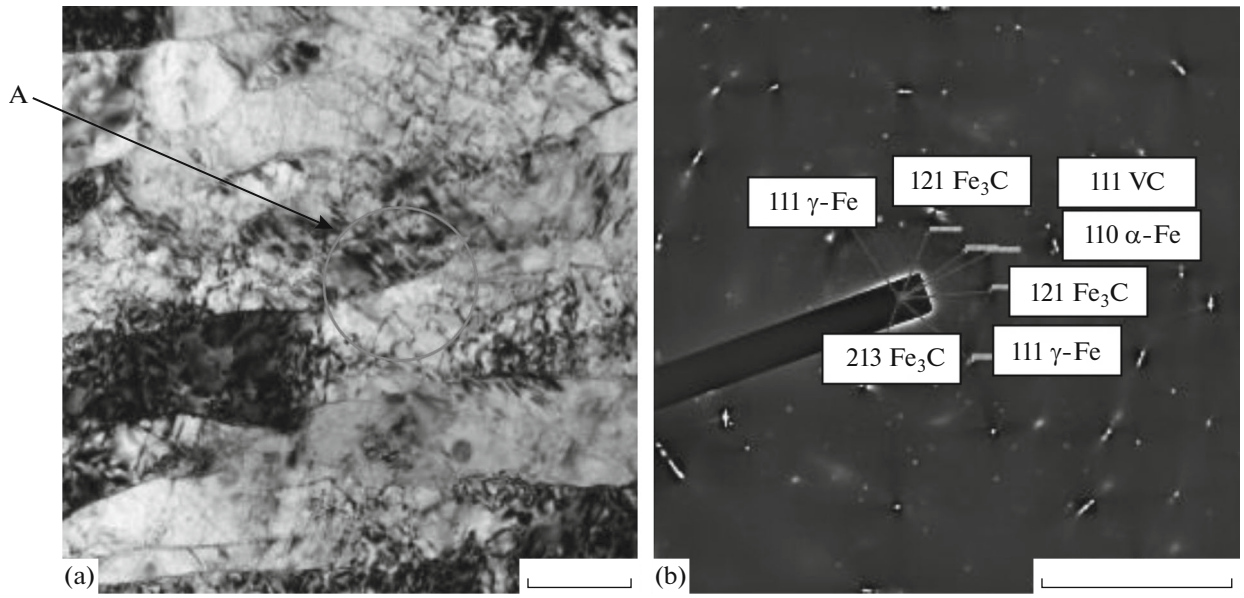

Fig. 5. (a) Microstructure of initially quenched 08G2B steel after heating to $T_h = 650°C$ ($\tau_{hold} = 30$ min) and (b) electron diffraction pattern from area A according to TEM data.

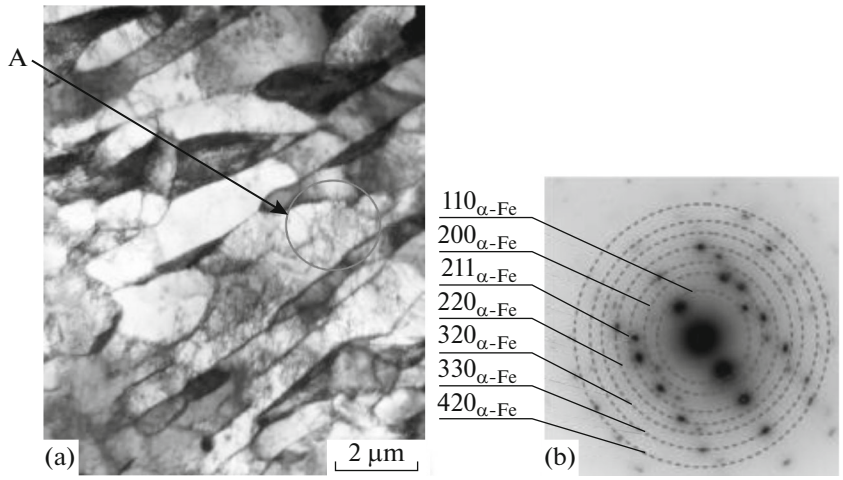

Fig. 6. (a) Microstructure of 08G2B steel after quenching in water ($T_h = 1000°C$) with subsequent heating to $T_h = 760°C$ ($\tau_{hold} =$ 30 min), water; (b) electron diffraction pattern from area A.

ery of grains, where low-temperature decomposition products are formed.

The austenite formed in the course of heating to $T_h = 850°C$ transforms into ferrite laths upon subsequent cooling of samples in water. In the structure, rounded particles of, probably, special carbides ~200 nm in size coagulated already in austenite and also, according to the microdiffraction patterns, Fe_3C particles precipitated upon cooling and residual austenite are observed.

In the 08G2B steel microstructure, after heating to $T_h = 900°C$ (close to Ac_3), as after the first quenching, there are laths of carbon-free bainite/martensite ≈0.15 μm in thickness; i.e., they are more dispersed than those after initial quenching. By electron diffraction, the presence of cementite and residual austenite is detected.

Therefore, after heating to Ac_1 and in the intercritical temperature range, in the initially quenched 08G2B steel, the dispersed lath structure with elevated dislocation density is preserved. It is obvious that this is a result of the inheritance of the lath structure by austenite from the initial quenching and the formation of displacive products of its decomposition upon finishing cooling. The high thermal stability of defects (dislocations and lath boundaries) in the studied steel

is unquestionably due to their strong fixation up to Ac_3 and a bit higher by dispersed particles of special carbides based on V, Nb, and Ti.

CONCLUSIONS

1. By dilatometric analysis, it was established that the temperature of the onset of austenite formation in ultrafine-grained 08G2B steel upon heating at a rate of $V_h = 90°C/s$ is $Ac_1 = 835°C$ and weakly depends on the initial state of the samples. The $\alpha \rightarrow \gamma$ reaction consists of two stages: a rapid low-temperature one from Ac_1 to $A_{tr} \approx 835°C$ and a decelerated high-temperature one in the range of A_{tr}–Ac_3, with $Ac_3 = 915°C$ for the initially quenched sample and 925°C for the normalized sample.

2. On the basis of the high-temperature X-ray diffraction investigations, it was determined that the first austenite portions have a high carbon content: 0.45 ± 0.02 and 0.25 ± 0.02 wt %, respectively, for the samples after quenching and normalization.

3. By scanning electron microscopy studies, it was established that first rounded austenite grains ~1.0 μm in size form along the grain boundaries of the initial α phase and, according to the data of X-ray spectrum microanalysis, have a chemical composition close to the average chemical composition of steel.

4. Using transmission electron microscopy, it was discovered that the lath structure with elevated dislocation density inherited from the quenched state is kept up to heating to the upper region of the intercritical temperature range, although, at as low as $T_h \geq 760°C$, migration of small areas of laths boundaries of the initial ferrite is observed.

REFERENCES

1. Oliveira, F.L.G., Andrade, M.S., and Cota, A.B. Kinetics of austenite formation during continuous heating in a low carbon steel, *Mater. Charact.*, 2007, vol. 58, pp. 256–261.
2. Asadi Asadabad, M., Goodarzi, M., and Kheirandish, S. Kinetics of austenite formation in dual phase steels, *ISIJ Int.*, 2008, vol. 48, pp. 1251–1255.
3. Zayats, L.Ts., Panov, D.O., Simonov, Yu.N., Balakhnin, A.N., Smirnov, A.I., and Yakovleva, I.L., Formation of austenite in initially quenched low-carbon steels of different alloying systems in the intercritical temperature interval, *Phys. Met. Metallogr.*, 2011, vol. 112, no. 5, pp. 480–487.
4. Makovetskii, A.N., Tabatchikova, T.I., Yakovleva, I.L., Tereshchenko, N.A., and Mirzaev, D.A., Structure formation in low-alloy pipe steel during heating in the intercritical temperature range, *Phys. Met. Metallogr.*, 2012, vol. 113, no. 7, pp. 704–715.
5. Farber, V.M., Khotinov, V.A., Selivanova, O.V., Polukhina, O.N., Yurovskikh, A.S., and Panov, D.O., Kinetics of formation of austenite and effect of heating in the intercritical temperature range on the structure of steel 08G2B, *Met. Sci. Heat Treat.*, 2017, vol. 58, no. 5, pp. 650–655.
6. Stepanov, A.I., Ashikhmina, I.N., Sergeeva, K.I., Belikov, S.V., Musikhin, S.A., Karabanalov, M.S., and Al-Katawi, A.A., Structure and properties of low-alloy Cr–Mo–V steel after austenitization in the intercritical temperature range, *Steel Transl.*, 2014, vol. 44, no. 6, pp. 469–473.
7. Vyboishchik, M.A., Marchenko, L.G., Grekhov, A.I., and Zhukova, S.Yu., Structure and properties of low-carbon steel pipes after intercritical interval quenching and tempering, *Tekhnol. Met.*, 2002, no. 12, pp. 22–25.
8. Skorokhodov, V.N., Odesskii, P.D., and Rudchenko, A.V., *Stroitel'naya stal'* (Steel for Building Industry), Moscow: Metallurgiya, 2002.
9. Maksimov, A.B. and Gulyaev, M.V., A hardening model for carbon and low-alloyed steels with a heterogeneous structure, *Materialovedenie*, 2016, no. 5, pp. 3–7.
10. Trotsan, A.I., Khlestov, V.M., Burova, D.V., and Khadzhinov, P.D., Microstructure and mechanical properties of 30KhGSA steel after energy-saving heat treatment with heating in the intercritical temperature interval, *Materialovedenie*, 2015, no. 6, pp. 8–14.
11. Christian, J.W., *The Theory of Transformations in Metals and Alloys*, Oxford: Pergamon, 1965.

Translated by Z. Smirnova